

Article

Microstructural Investigations of Low Temperature Joining of Q&P Steels Using Ag Nanoparticles in Combination with Sn and SnAg as Activating Material

Susann Hausner ^{1,*}, Martin Franz-Xaver Wagner ²  and Guntram Wagner ¹ 

¹ Composites and Material Compounds Group, Chemnitz University of Technology, 09107 Chemnitz, Germany; guntram.wagner@mb.tu-chemnitz.de

² Materials Science Group, Chemnitz University of Technology, 09107 Chemnitz, Germany; martin.wagner@mb.tu-chemnitz.de

* Correspondence: susann.hausner@mb.tu-chemnitz.de

Received: 10 January 2019; Accepted: 1 February 2019; Published: 6 February 2019



Abstract: Quenching and partitioning (Q&P) steels show a good balance between strength and ductility due to a special heat treatment that allows to adjust a microstructure of martensite with a fraction of stabilized retained austenite. The final heat treatment step is performed at low temperatures. Therefore, joining of Q&P steels is a big challenge. On the one hand, a low joining temperature is necessary in order not to influence the adjusted microstructure; on the other hand, high joint strengths are required. In this study, joining of Q&P steels with Ag nanoparticles is investigated. Due to the nano-effect, high-strength and temperature-resistant joints can be produced at low temperatures with nanoparticles, which meets the contradictory requirements for joining of Q&P steels. In addition to the Ag nanoparticles, activating materials (SnAg and Sn) are used at the interface to achieve an improved bonding to the steel substrate. The results show that the activating materials play an important role in the successful formation of joints. Only with the activating materials, can joints be produced. Due to the low joining temperature (max. 237 °C), the microstructure of the Q&P steel is hardly influenced.

Keywords: low temperature joining; nano-joining; silver sintering; alternative brazing; alternative soldering; Q&P steels; activating material; SnAg solder; Sn foil; Sn PVD coating

1. Introduction

Quenching and partitioning (Q&P) steels are C–Mn–Si multiphase steels with an excellent balance between strength and ductility, which receive their properties from a special heat treatment consisting of a Q&P process. These steels are very interesting for lightweight and safe automotive structures [1] and have been intensively investigated in recent years. Quenching and partitioning steels close the gap between the first generation of advanced high-strength steels (AHSS), such as dual phase (DP) steels, complex phase (CP) steels, martensitic (MART) steels or transformation induced plasticity (TRIP) steels and the second generation of AHSS, such as twinning-induced plasticity (TWIP) steels or Al-added lightweight steels with induced plasticity (L-IP), see Figure 1. Significant advantages of Q&P steels include (i) a reduced amount of alloying elements and thus lower costs in comparison to second generation AHSS, and (ii) improved mechanical properties compared to first generation AHSS, see Figure 1 [2,3]. Therefore, Q&P steels represent a promising approach for the third generation of AHSS [3].

With the Q&P process, the amount of martensite and retained austenite can be adjusted. Figure 2 illustrates a typical T-t-regime of such a Q&P process. After austenitization, the first process step (quenching) is rapid cooling to a quenching temperature (T_q) between the martensite-start temperature (M_s) and the martensite-finish temperature (M_f), which results in a well-defined microstructure of martensite and austenite. In the second step (partitioning), an isothermal holding at T_q (one-step Q&P) or above T_q (two-step Q&P) is performed. This leads to carbon diffusion from the supersaturated martensite into austenite, resulting in a stabilization of austenite after subsequent cooling to room temperature and in a reduction of internal stresses in the martensite phase [2,4–7]. The formation of carbides during this heat treatment is inhibited due to alloying with Si or Al [4,8].

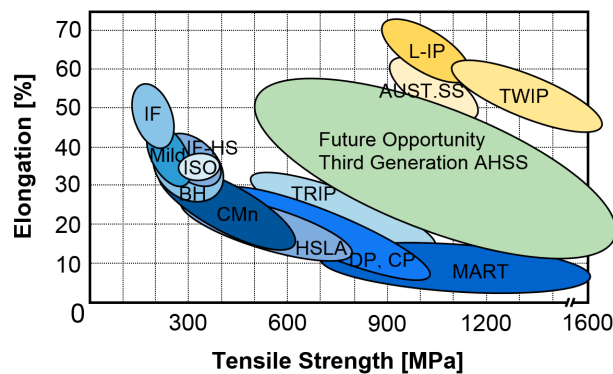


Figure 1. Tensile elongations and strengths for the first generation of advanced high-strength steels (AHSS) (lower-right) and second generation (upper-right) with a gap in between, representing the opportunity for the third generation of AHSS, according to References [2,3].

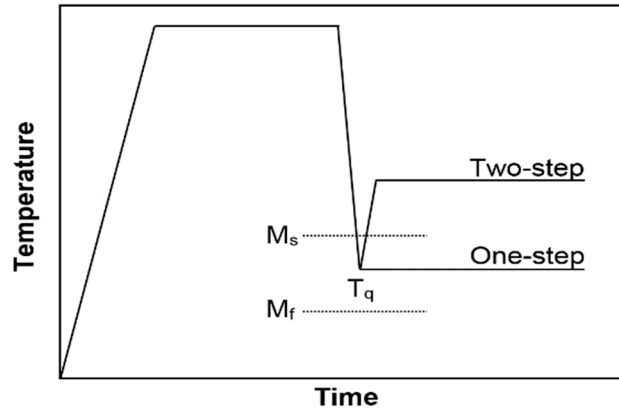


Figure 2. Schematic T-t-regime of a Quenching and partitioning (Q&P) process.

With this heat treatment, which was first proposed by Speer et al. [4], a microstructure of martensite with a well-defined fraction of retained austenite can be obtained. This results in a good balance between high strength (1000–1400 MPa [9]) and ductility (10–20% [9]), and therefore in a mostly ductile fracture behavior. Depending on the selected temperatures (one-step or two-step Q&P) and holding times, the properties of the steel can be specifically influenced [2,5,6,10–12].

For an industrial application of Q&P steels, developments and investigations of joining methods is an important field. In previous studies, in particular, resistance spot welding, which is the primary method in automobile manufacturing [13], was investigated for joining [9,13–17]. It was shown that joining of Q&P steels by resistance spot welding is usually possible but that the microstructure of the Q&P steels is often entirely changed, resulting locally in a loss of the desired mechanical properties [13,14,17]. For example, in Reference [17] it was found that due to the welding process, the martensite exhibited a reduced hardness and the austenite was converted into bainite. Moreover,

alloying elements, for example P and B, in the steel can affect the weldability by forming inclusions in the fusion zone and undesirable phases in the heat-affected zone [14].

Since the multi-phase microstructure of the Q&P steel is essential for the balance in terms of strength and ductility, a modification of the microstructure during subsequent joining processes should be avoided. The last heat treatment step (partitioning) is performed at relatively low temperatures, for example at 250 °C in our own experiments, see Section 2.1. Therefore, joining of Q&P steels without influencing the microstructure is a big challenge. On the one hand, a low joining temperature is necessary in order not to influence the partitioned microstructure; on the other hand, high joint strengths are required. A new way of meeting these two contradictory requirements is joining with nanoparticles, which has been the subject of intensive research in recent years. Joining with nanoparticles exploits the effect that nanoparticles exhibit lower melting and sintering temperatures compared to the corresponding bulk material because of the large surface-to-volume ratio. This enables joining at lower temperatures. The main advantage is that after melting and sintering of the particles, i.e., after the joining process, the material possesses the properties of the bulk material so that high-strength and temperature-resistant joints can be produced at low temperatures. In addition, hybrid joints, such as metal–ceramic joints, can be produced in this way, which is not feasible with fusion welding processes. Until now, joining with nanoparticles has mostly been investigated as an alternative for electronic packaging, i.e., for components subjected to low mechanical stresses [18–23]. However, our own recent studies show that joining with nanoparticles is also suitable for components subjected to high mechanical loads if suitable process parameters are used [24–26]. In summary, joining with nanoparticles represents an interesting alternative to perform joining processes at low temperatures, which allows to maintain the specific microstructure and mechanical properties of Q&P steels. In the present study, joining of Q&P steels using Ag nanoparticles is investigated. As a novelty, additional activating materials (SnAg and Sn) were used at the interface to achieve an improved bonding to the steel substrates.

2. Materials and Methods

2.1. Steel Composition and Heat Treatment

The chemical composition of the used steel is summarized in Table 1. The high Si content prevents the formation of carbides [8]. For the Q&P heat treatment, sheets with a thickness of 10 mm were heat-treated according to the temperature–time regime shown in Figure 3. Austenitization was performed at 950 °C. After quenching to 350 °C in water, the sheets were further cooled down to 150 °C in a molten salt bath. This was followed by a dwell time of 5 min in the salt bath (150 °C). Partitioning was performed at a temperature of 250 °C, first by heating to 250 °C over a period of 35 min and finally by holding at this temperature for 10 min. Cooling to room temperature took place in air. With this heat treatment, high strength, and good ductility can be achieved in this Q&P steel, as documented by an ultimate tensile strength and fracture strain of $R_m = 1970$ MPa and $A_5 = 13.7\%$, respectively [27]. The samples for joining tests were cut from the heat-treated sheets using electric discharge machining. The sample geometry is shown schematically in Figure 4.

Table 1. Composition of the Q&P steel determined by glow-discharge optical emission spectroscopy.

Element	C	Si	Mn	P	S	Cr	Ni	Mo	Cu	W	Al	Nb	Fe
wt%	0.41	1.95	0.68	0.01	0.006	1.34	0.036	0.04	0.003	0.008	0.009	0.068	Bal.

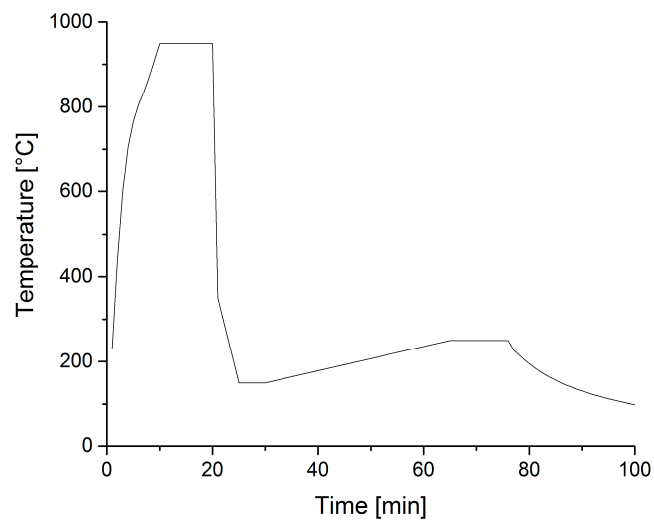


Figure 3. T-t-regime of the heat treatment used for preparation of all Q&P steel samples.

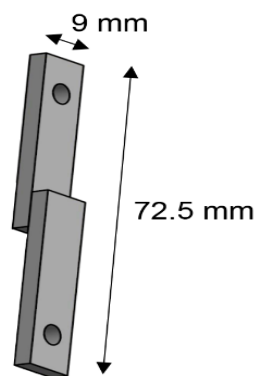


Figure 4. Sample geometry for joining experiments. Overlap: 7.5 mm, sheet thickness: 3 mm.

2.2. Joining Experiments

For joining, the heating of the samples was carried out in air by means of induction. The influence of different materials and process variations on the microstructure of the joints was investigated. Different nanopastes were used, in which the nanoparticles are suspended in solvents. Moreover, dispersing agents were added because they can prevent agglomeration of the particles.

A first series of experiments was performed with a Ni nanopaste. The composition of this paste, which was custom-made, is shown in Table 2. The preparation of the paste is described in Reference [26]. For joining with this nanopaste, a joining temperature of 650 °C, a joining pressure of 20 MPa, and a holding time of 10 min were used.

Table 2. Composition of the Ni nanopaste.

Particle size [nm]	Ni	10–100
Metal content [wt%]	Ni	49.0
Content of organic substances [wt%]	α -Terpineol	24.5
	p-Xylene	24.5
	1-Tetradecanethiol ($\text{CH}_3(\text{CH}_2)_{13}\text{SH}$)	1.0
	1-Octadecanethiol ($\text{CH}_3(\text{CH}_2)_{17}\text{SH}$)	1.0

In further experiments, a commercially available Ag nanopaste (Harima Chemicals, Inc., Nagoya, Japan) was used for joining. The composition of the Ag nanopaste is shown in Table 3. Joining with this paste has already been investigated in References [24,25]. For joining with this nanopaste, temperatures of 250 °C and 300 °C were tested with a holding time of 10 min and a joining pressure of 40 MPa.

Table 3. Composition of the Ag nanopaste (manufacturer’s specification).

Particle size [nm]	Ag	8–15
Metal content	Ag	82.1
Content of organic substances [wt%]	1-Decanol	1–2
	Petroleum hydrocarbon	2.5–3.5
	Dispersant A	6–10
	Dispersant B	1–3
	Additives A	2–3
	Additives B	0.8–1.5

Furthermore, in addition to the Ag nanopaste, low-melting materials were used at the edges of the substrates as an activating material to achieve an improved bonding. The enhanced bonding in this case was obtained by the melting process of the activating material, in contrast to the use of nanomaterials that usually only bind by sintering processes, i.e., in a solid phase process [24,25]. The use of activating materials results in a kind of sandwich structure of the joining seam (as shown schematically in Figure 5). The activating material only needs to fulfill the function of bonding between filler material and substrate and should therefore be as thin as possible. In contrast, the Ag nanopaste should be thicker than the activating material since the significantly improved properties of Ag, in particular strength and thermal stability, shall dominate the properties of the joining seam. It was also envisaged that the molten material could fill the pores that were formed by the sintering process of the nanopaste [24,25]. Thus, a denser joining seam might be achieved, which would have a positive effect on the strength of the joints.

In a first step, various SnAg solders were examined as activating material. The solders (available in the initial state as wire) were rolled into foils with thicknesses of approximately 20 µm, so that the foils could be applied directly on the surface of the substrate. For the experiments, three different solders with and without flux and with different holding times were tested (Table 4). The joining temperature was 230 °C, and thus below the last step of the Q&P heat treatment, so that an influence on the steel’s microstructure is unlikely.

In the second step, pure Sn wires were rolled into foils with a thickness of approximately 20 µm and were used as activating material with an increased joining temperature of 237 °C. In addition, different holding times and various thicknesses of the nanopastes were tested, see also Table 4.

For preparation of the specimens, the Ag nanopaste was applied on one side of the foils (Sn and SnAg) with the thickness given in Table 4 using a screen-printing process. All joining tests with the activating materials were performed without pressure. The specifications of the activating materials and the corresponding parameters for the joining tests are summarized in Table 4.

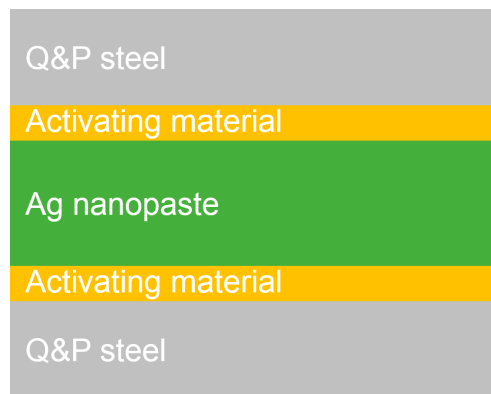


Figure 5. Structure of the joining seam (schematic) with the use of activating materials before joining.

Table 4. Specifications of the activating materials and parameters used for the joining process.

Activating Material	Flux (According to DIN EN ISO 9454-1)	Parameters for Joining		
		Temperature	Holding Time	Thickness of Paste Application
Solder SnAg3.5	Without flux	230 °C	30 min	20 µm
Solder SnAg4	2.2.3	230 °C	10 min	20 µm
Solder SnAg5	2.2.2	230 °C	10 min	20 µm
Sn (purity: 99.5 wt%)	Without flux	237 °C	3 min	40 µm
			5 min	80 µm

In a third step, Sn coatings were applied to the Q&P substrates using physical vapor deposition (PVD). The aim was to realize thinner Sn layers compared to the foils. Layer thicknesses of 3 µm, 10 µm, and 20 µm were investigated (Table 5). At a joining temperature of 237 °C, holding times of 3 min and 5 min were examined (Table 5). The Ag nanopaste was applied on one side of the PVD coating with a thickness of 20 µm. Joining was carried out without pressure.

Table 5. Parameters for the joining process using physical vapor deposition (PVD) Sn coatings.

Thickness of PVD Sn Coating	Joining Temperature	Holding Time	Thickness of Paste Application
3 µm 10 µm 20 µm	237 °C	3 min 5 min	20 µm

All joints were investigated regarding to the resulting microstructure. A light microscope (OLYMPUS GX51) and a scanning electron microscope (SEM, NEON40EsB) were used.

3. Results and Discussion

3.1. Joining without Activating Materials

For joining without activating materials, a Ni nanopaste and an Ag nanopaste were used. Relatively high temperatures of at least 650 °C are required for joining with Ni nanopaste [26]. Even if an influence on the Q&P microstructure was to be expected when using such high joining temperatures, the basic feasibility of joining with a Ni Nanopaste should still be examined. Figure 6 shows that joining of the Q&P steel with a Ni nanopaste is basically possible (joining temperature: 650 °C, holding time: 10 min, joining pressure: 20 MPa). A bonding can be successfully achieved. However, the optical micrographs already show that the microstructure of the Q&P steel is influenced considerably by the

joining process (Figure 6) compared to the microstructure in the initial state (Figure 7). Therefore, joining of Q&P steels with the Ni nanopaste is not expedient.

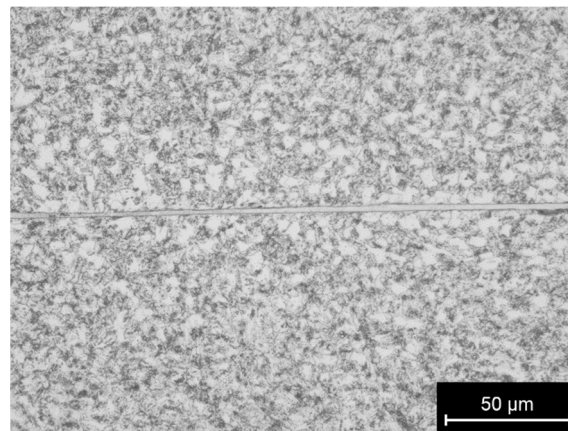


Figure 6. Light microscopy image of the Q&P steel joined with a Ni nanopaste (joining temperature: 650 °C, holding time: 10 min, joining pressure: 20 MPa).

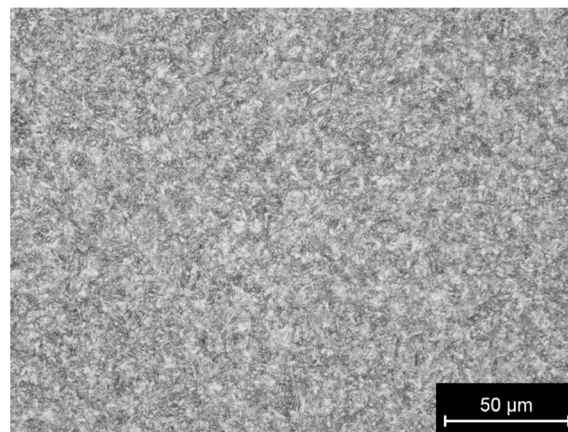


Figure 7. Light microscopy image of the Q&P steel in the initial state.

Therefore, in further experiments, joining with an Ag nanopaste was investigated, which allows for significantly lower joining temperatures [24,25]. Joining tests with the Ag nanopaste were carried out at temperatures of 250 °C and 300 °C with a holding time of 10 min and a joining pressure of 40 MPa. These parameters have been successfully used to join copper as substrate [24,25]. However, when using Q&P steel as substrate, no bonding could be achieved. This is most likely a consequence of the immiscibility of Ag and Fe. Moreover, when joining with nanoparticles, sintering processes have a bigger influence than melting processes [24,25], so that diffusion is limited. Therefore, the addition of different activating materials was investigated in further experiments, which were supposed to lead to an improved bonding between filler material and substrate.

3.2. Joining with Activating Materials

3.2.1. Joining with SnAg Solders as Activating Material

Low melting materials were used as activating material in combination with the Ag nanopaste to achieve an enhanced bonding through melting of the activating material and miscibility between substrate and activating material. In a first step, SnAg solders were investigated as activating materials. Three different solders with and without flux were tested (Table 4). Joining was again carried out at a temperature of 230 °C, i.e., below the last step of the Q&P heat treatment. For the joining experiments,

different holding times were tested (Table 4). The joining process with the activating materials was performed without pressure.

Figures 8–10 show optical micrographs of the joints with the different solders. The micrographs demonstrate that bonding can be achieved with all three solders. When using the solder SnAg3.5 without flux (Figure 8), a comparatively long holding time of 30 min was chosen to achieve a sufficiently good bonding to the Q&P steel even without flux. However, this long holding time leads to a distinctive formation of intermetallic compounds (IMC) in the joining seam. On the one hand, EDX analyses show that these are the typical Ag_3Sn phases (Figure 11). On the other hand, FeSn_2 phases also formed due to the long holding time, and thus the possibility of intensive diffusion between joining seam and substrate. Compared to Ag_3Sn , much more FeSn_2 phases formed. In comparison to the other two SnAg solders SnAg4 and SnAg5, where a short holding time of 10 min was used, with SnAg3.5 more IMC formed due to the long holding time of 30 min (Figures 8–10). Therefore, it must be assumed that the mechanical properties were negatively influenced when using a long holding time. In future investigations, an optimum holding time needs to be identified, with the goal of obtaining a minimized formation of IMC but also a sufficient bonding to the substrate.

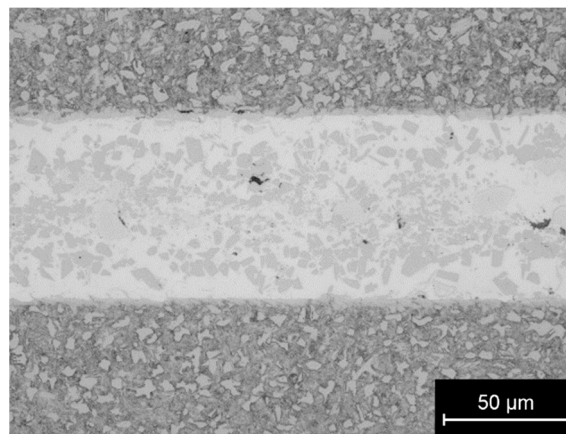


Figure 8. Light microscopy image of a joint with SnAg3.5 (without flux) (joining temperature: 230 °C, holding time: 30 min).

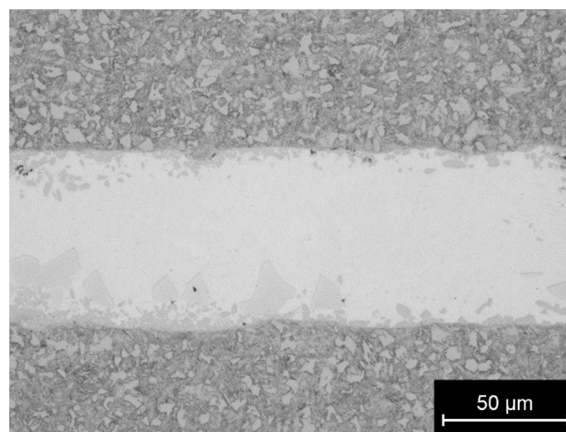


Figure 9. Light microscopy image of a joint with SnAg4 (with flux 2.2.3) (joining temperature: 230 °C, holding time: 10 min).

Figure 12, which depicts the interface between substrate and joining seam (solder: SnAg3.5), clearly shows that good bonding can be achieved even without flux. Pronounced diffusion processes take place between activating material and substrate—even in areas far from the substrate, the joining seam contains approximately 2 at% Fe. In the substrate, an interesting diffusion behavior along the

typical Q&P structure can be observed, Figure 12. Sn from the solder can be detected in the substrate up to a depth of approximately 4 μm . This pronounced diffusion indicates that the holding time can be reduced to minimize the formation of brittle phases. Therefore, in further tests the holding time was varied (see Section 3.2.2) to achieve an optimum between minimized formation of IMC and sufficient bonding.

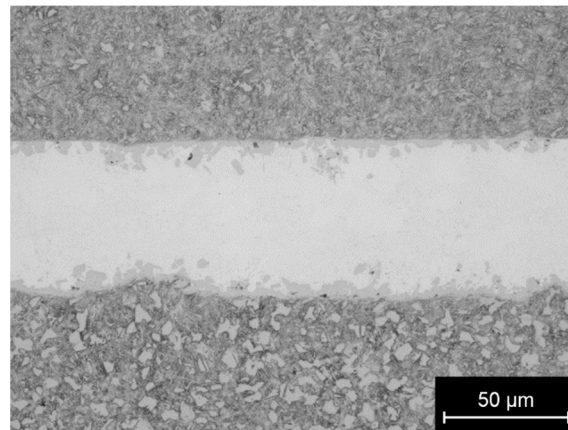


Figure 10. Light microscopy image of a joint with SnAg5 (with flux 2.2.2; joining temperature: 230 °C, holding time: 10 min).

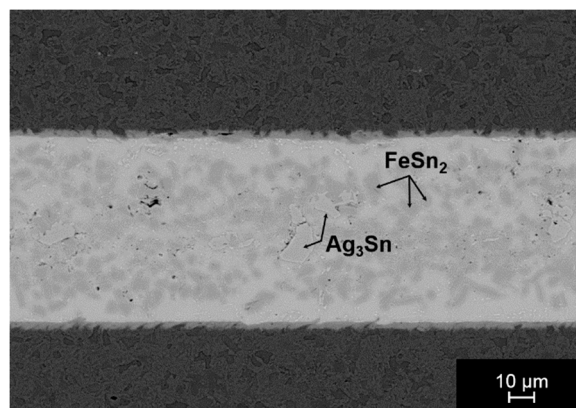


Figure 11. SEM image of a joint with SnAg3.5 as activating material (without flux; joining temperature: 230 °C, holding time of 30 min).

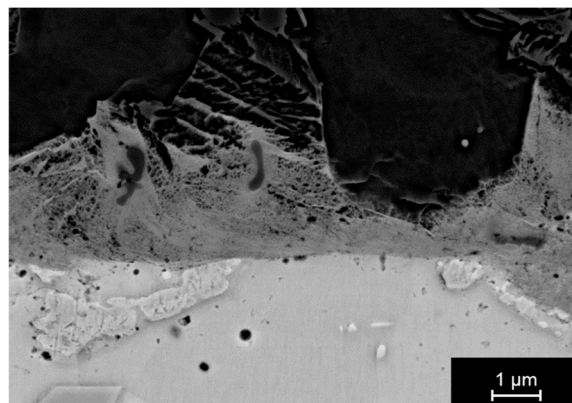


Figure 12. SEM image of the interface between the Q&P steel and the joining seam (activating material: SnAg3.5, without flux; joining temperature: 230 °C, holding time: 30 min).

The marks in Figure 13 show residues of the Ag sintered seam (activating material: SnAg3.5). Contrary to the assumption that the molten solder might fill the pores of the sintered seam, the sintered Ag material is distributed in the liquid solder. In addition, Ag does not dominate the joining seam. The Ag nanopaste was applied with a thickness of 20 μm , because this paste thickness was determined as an optimum for sintering [24]. The sintering process obviously causes shrinkage of the Ag material, leaving behind an even thinner Ag layer. The rolled solder foils had a thickness of approx. 20 μm . A rolling out to thinner foils was not possible with the available rolling mill. Since the properties of the solder dominate the joining seam with this thickness ratio between solder and nanopaste, a thicker paste application was tested in further investigations (see also Section 3.2.2).

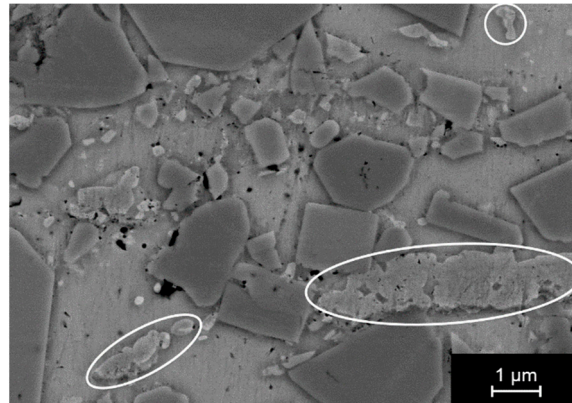


Figure 13. SEM image of the joining seam with SnAg3.5 as activating material (without flux) with residues of the Ag sintered seam (joining temperature: 230 °C, holding time: 30 min).

With the solders SnAg4 and SnAg5, a significantly reduced formation of brittle phases can be observed due to the shorter holding time of 10 min, where the IMC were formed primarily at the edges of the joining seam (Figures 9 and 10). The experiments demonstrated that good bonding to the substrates can also be achieved with these solders. Despite the shortened holding time of 10 min, the diffusion depths (up to 3 μm , Figures 14 and 15) are comparable with those of joining experiments with 30 min holding time (Figure 12). However, further tests showed that the flux contained in these two solders (2.2.3 in SnAg4 and 2.2.2 in SnAg5) is of critical importance for good bonding. If pure Sn foils are used without flux and the same holding time of 10 min, no comparable diffusion depths can be achieved (see Section 3.2.2).

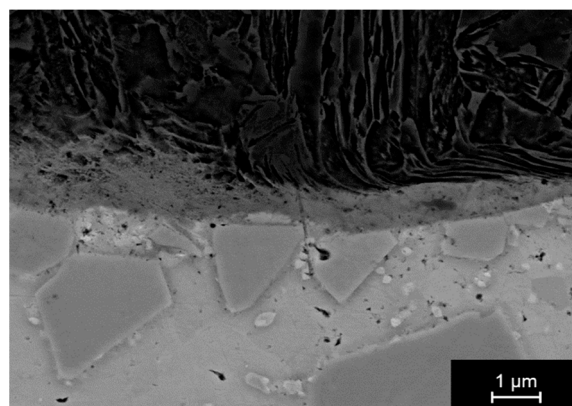


Figure 14. SEM image of the interface between the Q&P steel and the joining seam (activating material: SnAg4, with flux 2.2.3; joining temperature: 230 °C, holding time: 10 min).

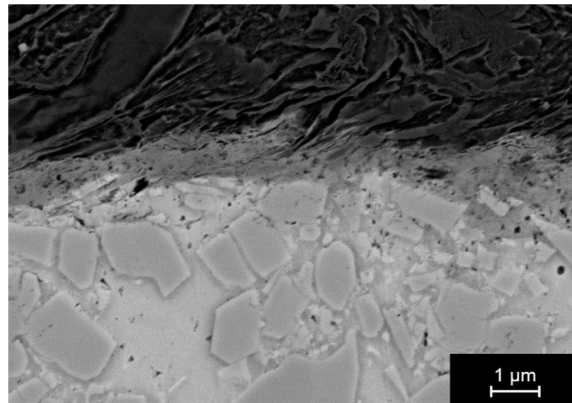


Figure 15. SEM image of the interface between the Q&P steel and the joining seam (activating material: SnAg5, with flux 2.2.2; joining temperature: 230 °C, holding time: 10 min).

After joining, the substrate exhibits the typical features of a predominantly martensitic, Q&P microstructure, Figure 16. This indicates that the joining process (solder: SnAg4, temperature: 230 °C, holding time: 10 min) only leads to negligible microstructural changes. Further work, particularly mechanical testing and additional microstructural analysis, is required to fully support this hypothesis.

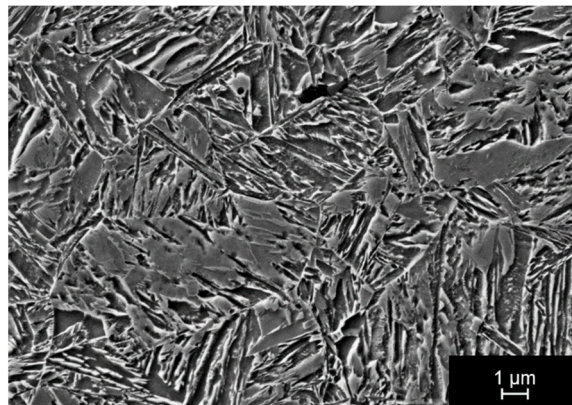


Figure 16. SEM image of the Q&P steel substrate after joining with SnAg4 at 230 °C with a holding time of 10 min.

3.2.2. Joining with Sn as Activating Material

Due to the formation of brittle phases when using the solders, the use of pure Sn as activating material was tested in further experiments, especially to prevent formation of Ag_3Sn . In addition, the thickness of nanopaste application and the holding time were varied in these tests. When varying the thickness of paste application, the aim was to provide as much Ag as possible in the joining seam compared to Sn, so that Ag dominates the properties of the joining seam. A paste application of 40 μm and 80 μm in combination with a Sn foil thickness of 20 μm was tested. The purpose of varying the holding time was to find an optimum time to minimize the formation of the brittle phases $FeSn_2$. Simultaneously, the aim was to achieve a good bonding as well as diffusion between joining seam and substrate even without flux. Holding times of 3 min and 5 min were investigated. Due to the use of pure Sn, the joining temperature was increased to 237 °C (compared to 230 °C when using the solders), Table 4.

Figure 17 shows an SEM image of the joining seam with a holding time of 5 min and a paste application of 40 μm . In comparison to a holding time of 30 min (Figure 8), in which the $FeSn_2$ phases are distributed over the entire joining seam, these phases are only formed at the edges of the joining seam when using a holding time of 5 min. In addition, a significantly smaller number of $FeSn_2$

precipitates are formed compared to a holding time of 10 min (Figures 9 and 10). However, as can be seen in Figure 17, despite the use of a pure Sn foil, Ag_3Sn is formed in the joining seam. It must be assumed that these phases are formed extremely quickly due to the presence of Ag from the nanopaste. Furthermore, the matrix consists of a Sn–Ag eutectic (Sn:Ag 94:6 at%), Figure 17. Thus, Ag from the nanopaste is “used up” for the formation of Ag_3Sn and the eutectic microstructure. Consequently, no high Ag content was available in the joining seam, which was actually expected as an important factor to obtain good mechanical properties for the joint.

Figure 18 shows the interface between joining seam and substrate with a holding time of 5 min. Compared to the microstructure after a holding time of 10 min (Figures 14 and 15), the diffusion zone with a depth of up to 0.5 μm was significantly thinner. Further work on the effect of the thinner diffusion zone on the mechanical properties is currently under way.

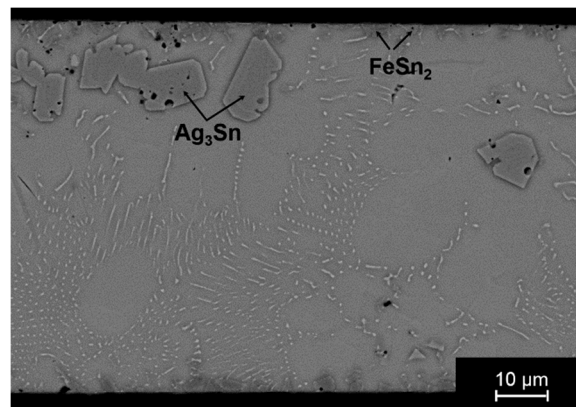


Figure 17. SEM image of a joint with Sn as activating material and a thickness of Ag nanopaste application of 40 μm (joining temperature: 237 $^\circ\text{C}$, holding time: 5 min).

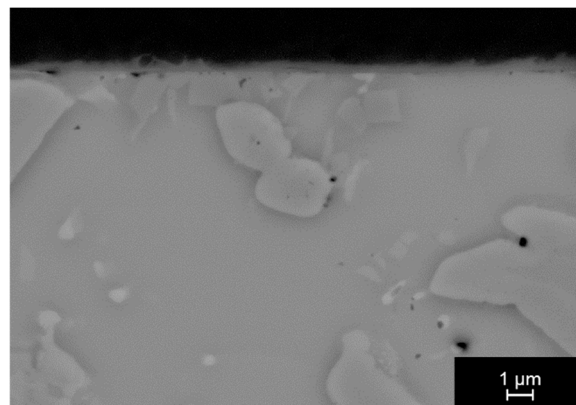


Figure 18. SEM image of the interface between the Q&P steel and the joining seam (activating material: Sn; joining temperature: 237 $^\circ\text{C}$, holding time: 5 min).

With a paste application of 80 μm , an increased porosity was observed in the joining seam, which was a result of the thick paste application. A thick application of nanopaste inevitably leads to an increased evaporation of organic substances, and therefore to a higher porosity, which was already observed previously [24]. In this work, an optimum paste application of 20 μm was determined, in which the porosity was “acceptable”, because it was low and finely distributed. The application of 20- μm paste was already tested with the SnAg solders but was not suitable due to the lack of options for rolling foils with a thickness of < 20 μm , which is a requirement for the properties of Ag to dominate the joining seam. Accordingly, the goal of further work was to apply thinner Sn layers to the substrates, which would also allow a thinner application of the Ag nanopaste.

Therefore, in further tests, Sn PVD coatings of the Q&P substrates were examined, because via PVD significantly thinner Sn layers can be deposited. Sn layer thicknesses of 3 μm , 10 μm , and 20 μm were tested with a constant nanopaste application of 20 μm (Table 5). During the experiments, a further advantage was recognized when using the PVD layers. The nanopaste can be applied more easily to the rigid coatings than to the flexible foils.

Indeed, several interesting phenomena, which cannot be fully explained yet, were observed when using the PVD coatings. Whisker formation in the joining seams was often observed (Figures 19 and 20). Such whisker growth is known from the use of lead-free Sn solders with copper substrates [28]. It is assumed that in particular external or internal stresses lead to the formation of whiskers. Often, intermetallic phases (IMC), especially Cu_6Sn_5 , were identified as starting point for the formation of whiskers [28], but also oxide layers on the surface can initiate whisker growth [29]. This whisker formation and growth is not completely understood and discussed controversially in the literature [28]. Also, in the present work, it could not be clarified why whisker formation suddenly starts when using the PVD Sn layers, because the whisker formation was not observed when using Sn foils with the same thickness of 20 μm . Intermetallic phases do not seem to be the starting point for whisker growth, since neither Ag_3Sn nor FeSn_2 are formed when using the PVD Sn layers (Figure 19). In contrast, IMC were observed with the same holding time (5 min) and the same Sn thickness (20 μm) when using Sn foils (Figure 17). Moreover, when using PVD Sn coatings, the joining seam exhibits a completely different microstructure of the matrix compared to the microstructure when using foils: With the same parameters ($T = 237^\circ\text{C}$, $t = 5$ min, Sn thickness = 20 μm), no eutectic structure formed when using the PVD coating (Figure 17 vs. Figure 19). In addition, the Ag was not used for the formation of Ag_3Sn , as it was observed when using the foils. Instead, sintered Ag particles were distributed within the joining seam (Figure 21). A gap remained in the middle of the joining seam, where the Ag nanopaste was applied (Figure 19). The Sn layers did not melt together sufficiently, which was likely to have a negative effect on the mechanical properties of these joints. A solution to this issue would be the application of light pressure during the joining process, or a slightly increased joining temperature.

The differences in the formation of the microstructure—no eutectic, no IMC—when using PVD coatings compared to the use of foils with otherwise identical process parameters cannot be explained yet and requires further in-depth studies. In principle, the changed formation of the microstructure can be considered as positive, since Ag is not used up for IMC formation, and therefore, Ag is available in the joining seam. The variations of the Sn layer thickness show that a 10- μm layer is still too thick, since the proportion of Ag in the joining seam is still lower compared to Sn (Figure 21). In contrast, with a coating thickness of 3 μm , the joining seam exhibits a high porosity, Figure 22. The proportion of Sn does not seem to be sufficient to fill the pores that are inevitably formed when using the nanopaste. Therefore, an optimum thickness of the Sn layer should be determined in further experiments. This means, on the one hand, that the layer should be thin enough so that Ag dominates the properties of the joining seam, and on the other hand, a sufficient amount of Sn should be available to fill the pores in the joining seam.

In addition, the interface between joining seam and substrate must be optimized in further tests. Despite using the same surface treatments (i.e., grinding and ultrasonic degreasing in acetone), bonding of the samples with the PVD layer is significantly deteriorated compared to those with the foils. When using the foils, a thin, yet clearly visible diffusion zone in the Q&P steel can be observed with a holding time of 5 min, Figure 18. In contrast, when using PVD layers, no diffusion zone can be observed, regardless of holding time and Sn thickness. Bonding to the substrate appears insufficient. In some cases, a gap was observed at the interface between substrate and joining seam, (see Figures 19, 21 and 22). In principle, it should be noted that with a short holding time, flux should probably be used for sufficient bonding, due to the significantly improved bonding when using the solders with flux (Figures 14 and 15). However, this must be confirmed with strength tests.

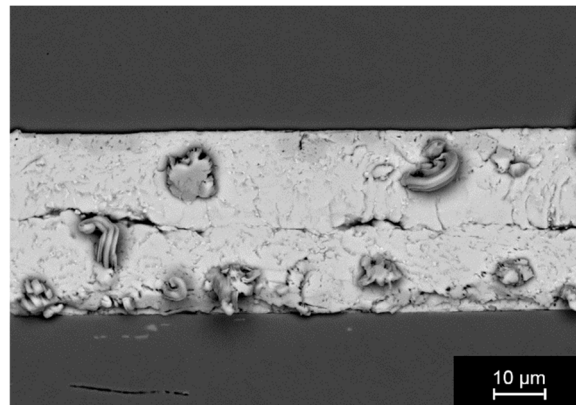


Figure 19. SEM image of a joint with PVD Sn coating (20 μm) as activating material (joining temperature: 237 °C, holding time: 5 min).

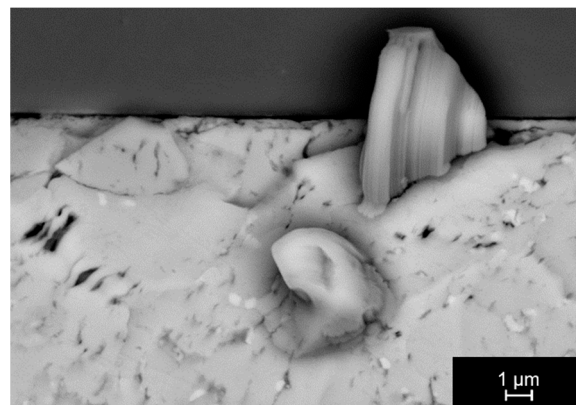


Figure 20. SEM image of a joint with PVD Sn coating (10 μm) as activating material (joining temperature: 237 °C, holding time: 5 min).

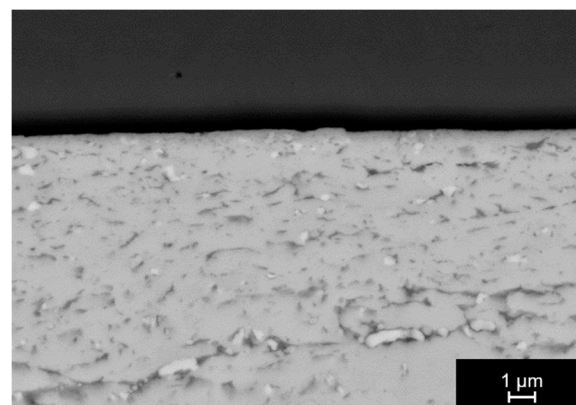


Figure 21. SEM image of a joint with PVD Sn coating (10 μm) as activating material (joining temperature: 237 °C, holding time: 3 min).

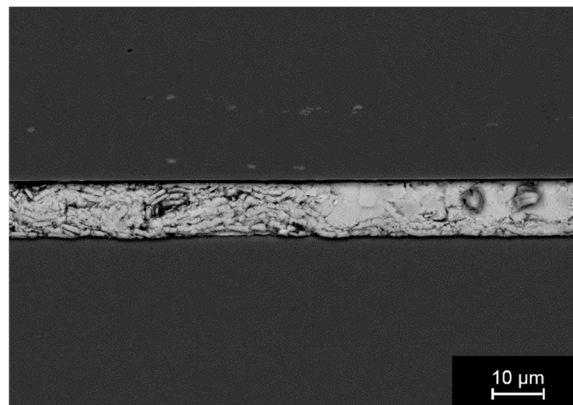


Figure 22. SEM image of a joint with PVD Sn coating (3 μm) as activating material (joining temperature: 237 $^{\circ}\text{C}$, holding time: 5 min).

4. Conclusions

The results show that the activating materials are a key factor for successful bonding to the Q&P steels. Using only the Ag nanopaste, no bonding can be achieved, whereas the combination of Ag nanopaste and activating materials (SnAg or Sn) leads to successful formation of joints. Due to the melting of the activating material and its miscibility with the steel substrate, a pronounced diffusion between joining seam and substrate can be observed when using foils as activating material. Due to the low joining temperatures (max. 237 $^{\circ}\text{C}$), the microstructure of the steel was hardly influenced by the joining process, which is important to maintain the excellent mechanical properties of the Q&P steel.

During the investigations, two main challenges have been identified when joining with activating materials in combination with the Ag nanopaste: (i) an optimal thickness ratio between the activating material and the Ag nanopaste must be determined, where a good bonding to the substrate is to be ensured, but at the same time the Ag from the nanopaste should dominate the properties of the joining seam; and (ii) an optimal holding time must be found with which the formation of IMC in the joining seam can be minimized, but nevertheless sufficient bonding to the substrate can be achieved.

For different types of activating material (foils vs. PVD coatings), pronounced differences in the microstructure of the joining seam were observed even when using otherwise identical process parameters. These differences cannot be explained completely yet and require additional in-depth studies. Moreover, the influence of different process variations on the mechanical strength of the joints should be investigated.

Author Contributions: Conceptualization, S.H., M.F.-X.W. and G.W.; Methodology, S.H., G.W.; Investigation, S.H., M.F.-X.W., G.W.; Writing—original draft preparation, S.H.; Writing—review and editing, S.H., M.F.-X.W., G.W.; Project Administration, M.F.-X.W.; Funding acquisition, S.H., G.W.

Funding: The publication costs of this article were funded by the German Research Foundation/DFG and the Technische Universität Chemnitz in the funding programme Open Access Publishing.

Acknowledgments: Andreas Gester is gratefully acknowledged for performing of the heat treatment.

Conflicts of Interest: The authors declare no conflict of interest.

References

1. Wang, L.; Feng, W. Development and Application of Q&P Sheet steels. In *Advanced Steels, Proceedings of the International Conference on Advanced Steels (ICAS), Guilin, China, 9–11 November 2010*; Weng, Y., Dong, H., Gan, Y., Eds.; Springer: Berlin/Heidelberg, Germany, 2011; pp. 255–258.
2. Speer, J.G.; De Moor, E.; Findley, K.O.; Matlock, D.K.; De Cooman, B.C.; Edmonds, D.V. Analysis of Microstructure Evolution in Quenching and Partitioning Automotive Sheet Steel. *Metall. Mater. Trans. A* **2011**, *42*, 3591–3601. [[CrossRef](#)]

3. Matlock, D.K.; Speer, J.G. Third generation of AHSS: microstructure design concepts. In *Microstructure and Texture in Steels and Other Materials*; Haldar, A., Suwas, S., Bhattacharjee, D., Eds.; Springer: London, UK, 2009; pp. 185–205.
4. Speer, J.G.; Matlock, D.K.; De Cooman, B.C.; Schroth, J.G. Influence of Interface Mobility on the Evolution of Austenite-Martensite Grain Assemblies during Annealing. *Acta Mater.* **2003**, *51*, 2611–2622. [[CrossRef](#)]
5. Speer, J.G.; Edmonds, D.V.; Rizzo, F.C.; Matlock, D.K. Partitioning of carbon from supersaturated plates of ferrite, with application to steel processing and fundamentals of the bainite transformation. *Curr. Opin. Solid State Mater. Sci.* **2004**, *8*, 219–237. [[CrossRef](#)]
6. Edmonds, D.V.; He, K.; Rizzo, F.C.; De Cooman, B.C.; Matlock, D.K.; Speer, J.G. Quenching and partitioning martensite—A novel steel heat treatment. *Mater. Sci. Eng. A* **2006**, *438*, 25–34. [[CrossRef](#)]
7. Mola, J.; De Cooman, B.C. Quenching and Partitioning (Q&P) Processing of Martensitic Stainless Steels. *Metall. Mater. Trans. A* **2013**, *44*, 946–967.
8. Gallagher, M.F.; Speer, J.G.; Matlock, D.K. Microstructure Development in TRIP-Sheet Steels Containing Si, Al, and P. In Proceedings of the 44th Mechanical Working and Steel Processing (MWSP) Conference, Orlando, FL, USA, 8–11 September 2002; Volume XL, pp. 153–172.
9. Wang, L.; Speer, J.G. Quenching and Partitioning Steel Heat Treatment. *Metallogr. Microstruct. Anal.* **2013**, *2*, 268–281. [[CrossRef](#)]
10. De Moor, E.; Lacroix, S.; Clarke, A.J.; Penning, J.; Speer, J.G. Effect of Retained Austenite Stabilized via Quench and Partitioning on the Strain Hardening of Martensitic Steels. *Metall. Mater. Trans. A* **2008**, *39*, 2586–2595. [[CrossRef](#)]
11. Santofimia, M.J.; Zhao, L.; Petrov, R.; Kwakernaak, C.; Sloof, W.G.; Sietsma, J. Microstructural development during the quenching and partitioning process in a newly designed low-carbon steel. *Acta Mater.* **2011**, *59*, 6059–6068. [[CrossRef](#)]
12. Sun, J.; Yu, H.; Wang, S.; Fan, Y. Study of microstructural evolution, microstructure-mechanical properties correlation and collaborative deformation-transformation behavior of quenching and partitioning (Q&P) steel. *Mater. Sci. Eng. A* **2014**, *596*, 89–97.
13. Wang, B.; Duan, Q.Q.; Yao, G.; Pang, J.C.; Li, X.W.; Wang, L.; Zhang, Z.F. Investigation on fatigue fracture behaviors of spot welded Q&P980 steel. *Int. J. Fatigue* **2014**, *66*, 20–28.
14. Amirthalingam, M.; Van der Aa, E.M.; Kwakernaak, C.; Hermans, M.J.M.; Richardson, I.M. Elemental segregation during resistance spot welding of boron containing advanced high strength steels. *Weld World* **2015**, *59*, 743–755. [[CrossRef](#)]
15. Ruso Spena, P.; De Maddis, M.; Lombardi, F. Mechanical strength and fracture of resistance spot welded advanced high strength steels. *Procedia Eng.* **2015**, *109*, 450–456. [[CrossRef](#)]
16. Fan, C.-L.; Ma, B.-H.; Chen, D.-N.; Wang, H.-R.; Ma, D.-F. Spall Strength of Resistance Spot Weld for QP Steel. *Chin. Phys. Lett.* **2016**, *33*, 036201:1–036201:5. [[CrossRef](#)]
17. Spena, P.R.; De Maddis, M.; D'Antonio, G.; Lombardi, F. Weldability and Monitoring of Resistance Spot Welding of Q&P and TRIP Steels. *Metals* **2016**, *6*, 270:1–270:15.
18. Guo, W.; Zhang, H.; Zhang, X.; Liu, L.; Peng, P.; Zou, G.; Zhou, Y.N. Preparation of nanoparticle and nanowire mixed pastes and their low temperature sintering. *J. Alloys Compd.* **2017**, *690*, 86–94. [[CrossRef](#)]
19. Siow, K.S.; Lin, Y.T. Identifying the Development State of Sintered Silver (Ag) as a Bonding Material in the Microelectronic Packaging Via a Patent Landscape Study. *J. Electron. Packag. Trans. ASME* **2016**, *138*, 020804. [[CrossRef](#)]
20. Peng, P.; Li, L.; Guo, W.; Hui, Z.; Fu, J.; Jin, C.; Liu, Y.; Zhu, Y. Room-Temperature Joining of Silver Nanoparticles Using Potassium Chloride Solution for Flexible Electrode Application. *J. Phys. Chem. C* **2018**, *122*, 2704–2711. [[CrossRef](#)]
21. Yan, H.; Mei, Y.; Li, X.; Chen, G.; Lu, G.-Q. A phase-leg IGBT module using DBC substrate without Ag finish by pressureless sintering of nanosilver paste. In Proceedings of the IEEE Applied Power Electronics Conference and Exposition (APEC 2017), Tampa, FL, USA, 26–30 March 2017; pp. 3013–3020.
22. Yao, T.; Matsuda, T.; Sano, T.; Morikawa, C.; Ohbuchi, A.; Yashiro, H.; Hirose, A. In Situ Study of Reduction Process of CuO Paste and Its Effect on Bondability of Cu-to-Cu Joints. *J. Electron. Mater.* **2018**, *47*, 2193–2197. [[CrossRef](#)]

23. Zhang, D.; Zou, G.; Liu, L.; Zhang, Y.; Yu, C.; Bai, H.; Zhou, N. Synthesis with glucose reduction method and low temperature sintering of ag-cu alloy nanoparticle pastes for electronic pack-aging. *Mater. Trans.* **2015**, *56*, 1252–1256. [[CrossRef](#)]
24. Hausner, S. Potential von Nanosuspensionen zum Fügen bei niedrigen Temperaturen. Ph.D. Thesis, Technische Universität Chemnitz, Chemnitz, Germany, 1 September 2015.
25. Hausner, S.; Weis, S.; Wielage, B.; Wagner, G. Low temperature joining of copper by Ag Nanopaste: Correlation of mechanical properties and process parameters. *Weld World* **2016**, *60*, 1277–1286. [[CrossRef](#)]
26. Hausner, S.; Weis, S.; Wagner, G. Joining of steels at low temperatures by Ni nanoparticles. *DVS-Berichte* **2016**, *325*, 278–284.
27. Mehner, T.; Scharf, I.; Frint, P.; Schubert, F.; Mašek, B.; Wagner, M.F.-X.; Lampke, T. Hydrogen embrittlement of a quenching and partitioning steel during corrosion and zinc electroplating. *Mater. Sci. Eng. A* **2019**, *744*, 247–254. [[CrossRef](#)]
28. Jadhav, N.; Chason, E. Sn Whiskers: Causes, Mechanisms and Mitigation Strategies. In *Lead-Free Solders: Materials Reliability for Electronics*; Subramanian, K.N., Ed.; John Wiley and Sons Ltd.: West Sussex, UK, 2012; pp. 299–321.
29. Sukanuma, K. Tin Whiskers. In *Lead-Free Solders: Materials Reliability for Electronics*; Subramanian, K.N., Ed.; John Wiley and Sons Ltd.: West Sussex, UK, 2012; pp. 323–335.



© 2019 by the authors. Licensee MDPI, Basel, Switzerland. This article is an open access article distributed under the terms and conditions of the Creative Commons Attribution (CC BY) license (<http://creativecommons.org/licenses/by/4.0/>).